Chitosan-based Peptidopolysaccharides as Cationic Antimicrobial Agents and Antibacterial Coatings

Dicky Pranantyo, Li Qun Xu, En-Tang Kang, and Mary B Chan-Park

Biomacromolecules, **Just Accepted Manuscript** • DOI: 10.1021/acs.biomac.8b00270 • Publication Date (Web): 19 Apr 2018

Chitosan-based Peptidopolysaccharides as Cationic Antimicrobial Agents and Antibacterial Coatings

Dicky Pranantyo[1], Li Qun Xu[1], En-Tang Kang[1]*, Mary B. Chan-Park[2]*

[1] Department of Chemical & Biomolecular Engineering
National University of Singapore
4 Engineering Drive 4, Kent Ridge
Singapore 117585

[2] Centre of Antimicrobial Bioengineering
School of Chemical and Biomedical Engineering
Nanyang Technological University
Singapore 637459

* Corresponding Authors
E-mail: cheket@nus.edu.sg (E.T.K)
mbechan@ntu.edu.sg (M.B.C.P)

* ORCID
En-Tang Kang: 0000-0003-0599-7834
Mary B. Chan-Park: 0000-0003-3761-7517

Abstract

The rapid spread of multidrug resistant bacteria has called for effective antimicrobial agents which work on a more direct mechanism of killing. Cationic peptidopolysaccharides are developed in the present work to mimic the peptidoglycan structure of bacteria and to enhance the membrane-compromising bactericidal efficacy. Antimicrobial CysHHC10 peptide was grafted to the C-2 (amino) or C-6 (hydroxyl) position of chitosan backbone via thiol-maleimide 'click' conjugation, utilizing the maleimidohexanoic linkers. The peptidopolysaccharide with primary amino backbone intact (CSOHHC) exhibited higher bactericidal activity towards Gram-positive and Gram-negative bacteria, in comparison to that with amino backbone grafted with the peptide (CSNHHC). Both peptidopolysaccharides also exhibited lower hemolytic activity and cytotoxicity than free CysHHC10 peptide due to the moderation effect contributed by the chitosan backbone. For targeting the Gram-positive bacteria in particular, the CSOHHC expressed four- and two-fold increases in hemo- and cytoselectivity, respectively, as compared to the CysHHC10 peptide. In an extended application, peptidopolysaccharide antibacterial coatings were formed via layer-by-layer assembly with tannic acid. The peptidopolysaccharide coatings readily killed the adhered bacteria upon contact while being cytocompatible by maintaining more than 60% viability for the adhered fibroblasts. Therefore, the peptidoglycan-mimetic peptidopolysaccharides are potential candidates for anti-infective drugs in biomedical applications.

Keywords: peptidopolysaccharide, chitosan, peptidoglycan-mimetic, antimicrobial peptide, antibacterial coating.

1. Introduction

In the era where the widespread exploitation of antibiotics has been exercised haphazardly, there is an overwhelming demand for the development of novel antimicrobial compounds in order to match the rapid growth of drug-resistant traits in clinically significant pathogens.[1] An alternative approach to reduce the propagation of drug-resistant evolvement is by employing cationic compounds to directly target the cytoplasmic membrane of bacteria. A library of cationic polymethacrylates,[2,3] polycarbonates,[4-6] polyamides,[7,8] polypyridines,[9] polynorbornenes,[10,11] and polypeptoids[12,13] have been developed to combat pathogenic bacteria. As an intrinsic part of the innate immune system in many organisms, cationic peptides have recently emerged as antimicrobial compounds with high killing potency towards a broad spectrum of bacteria due to the combined electrostatic effects and amphiphilic functions. Despite the minimum risk for inducing the resistant trait in bacteria, the applicability of antimicrobial peptides (AMPs) is limited by poor pharmacokinetics and proteolytic stability, as well as high toxicity towards blood and mammalian cells.[14] In addition to being disruptive towards plasma membrane of bacteria, cationic compounds also interrupt cells membrane of other organisms. Molecular design and engineering approaches have been carried out to prepare the next generation of AMPs that exhibit moderate toxicity and retain the membrane targeting ability. Conjugation of poly(ethylene glycol) (PEG) to the N-terminal of synthetic CaLL peptide comprising fragments of LL-37 and cecropin A peptides retained 50% microbial inhibitory concentration, which is 3-fold higher than free CaLL, while improving lung tissue compatibility following airway delivery.[15] Conjugation of cationic KSLW decapeptide to PEGylated phospholipid micelles also retained antimicrobial activity while inhibiting lipopolysaccharide-induced severe vascular inflammatory responses in human umbilical vein endothelial cells, as compared to the free peptide.[16]

Hyperbranched polyglycerols decorated with pendant aurein 2.2 peptide and its RW mutant, 77c peptide, demonstrated better cell and blood compatibilities, albeit lower antimicrobial activity, than the free peptides.[17,18]

Bacterial cell walls are different from those other organisms due to the presence of peptidoglycan, which is located immediately outside their cytoplasmic membrane. In Gram-positive bacteria, the peptidoglycan layer is substantially thicker than that in Gram-negative bacteria. This peptidoglycan consists of a polysaccharide backbone with pendent alternating residues of *N*-acetylmuramic acid and *N*-acetylglucosamine in equal amounts. Inspired by this structure, there is a growing interest to combine peptides with polysaccharide in order to recreate a peptidoglycan mimetic for targeting bacterial cell walls. A large number of polysaccharides are biocompatible in nature and therefore can also contribute to reducing the toxicity of cationic AMPs.[19] In particular, chitosan is a class of linear mucopolysaccharide comprising of D-glucosamine and *N*-acetyl-D-glucosamine derived from deacetylation of natural chitin, which is widely known for its hemocompatible, histocompatible, and biodegradable properties.[20] Molecular conjugation of chitosan with α- or ε-polylysines produced cationic peptidopolysaccharides which mimicked the peptidoglycan structures, resulting in higher selectivity towards bacteria as compared to mammalian cells.[21,22] Chitosan conjugated with AMP and gelatinase-cleavable peptide was reported to transform into a fibrous nanostructure upon reaching the bacterial infection site, exposing the AMP residues for multivalent cooperative electrostatic interactions with bacterial membranes.[23] Nisin was grafted to quaternary ammonium chitosan through an enzyme catalysed reaction to enhance its limited antimicrobial activity.[24] Conjugation of chitosan with anoplin, a decapeptide isolated from the venom of

solitary wasp, was also reported to enhance the antibacterial activity and hemocompatibility of the AMP.[25] However, almost all conjugations with peptides were carried out at the C-2 (amino) position of chitosan, and the structural configuration of these conjugates has one fundamental difference from the target peptidoglycan, which has pendent amino acid residues located on the C-3 (hydroxyl) position of its polysaccharide backbone.

In this study, maleimide-functionalized linkers were introduced to the C-2 or C-6 (hydroxyl) positions of chitosan backbone, which subsequently served as conjugation sites for cysteine-terminated HHC10 (KRWWKWIRW) AMP via thiol-maleimide 'click' chemistry (Scheme 1). The antimicrobial activity of HHC10 peptide has been confirmed in *in vitro* and *in vivo* tests,[26,27] and the 'clickability' of its cysteine-terminated form has been reported previously.[28] The resulting peptidopolysaccharide with the backbone amino groups intact was hypothesized to provide higher protonation capacity and water-solubility than that with the backbone amino groups grafted. Maleimide functionalization on the C-2 position of chitosan was carried out by maintaining continuous protection of the backbone primary amines in the protonating medium. Under this condition, there was a finite probability that the maleimide functionalization could also occur on the C-3 position of chitosan,[29] and subsequently led to a configuration more closely resembling the peptidoglycan structure. In addition, the intact amino groups of chitosan backbone could contribute additional electrostatic affinity to target the negatively charged surfaces of bacterial membrane. The antimicrobial activity towards Gram-positive and Gram-negative bacteria, hemocompatibility, and cytotoxicity of the two peptidopolysaccharides with different configurations were compared. To extend their potential applications,

antibacterial coatings of the peptidopolysaccharides were constructed via layer-by-layer assembly mediated by polyphenolic tannic acid. Bacteria adhesion assays were performed on the peptidopolysaccharide coatings to evaluate their antibacterial efficacy and cytocompatibility, the two important criteria for biomaterials application.

2. Experimental Section

2.1. Materials

Chitosan (CS, M_n 50–190 kD), 6-maleimidohexanoic acid (MIAc, 90%), oxalyl chloride (99%), *N*-(3-dimethylaminopropyl)-*N'*-ethylcarbodiimide (EDC, 97%), *N*-hydroxysuccinimide (NHS, 98%), methanesulfonic acid (99%), tannic acid (TA, ACS reagent), calcium chloride (93%), and methylthiazolyldiphenyl-tetrazolium bromide (MTT, 98%) were purchased from Sigma-Aldrich Chem. Co. (St. Louis, MO). CysHHC10 (H-CKRWWKWIRW-NH_2, 97%) peptide was purchased from China Peptides Co. Ltd. (Shanghai, China). Stainless steel (SS) foils (AISI type 304, 0.05 mm thick) were purchased from Goodfellow Ltd. (Cambridge, UK). Dichloromethane, dimethylformamide, dimethyl sulfoxide, and acetone were of analytical grade, while phosphate-buffered saline (PBS) was of ultrapure grade. *Escherichia coli* (*E. coli*, ATCC 25922), *Pseudomonas aeruginosa* (*P. aeruginosa*, ATCC 15692), *Staphylococcus aureus* (*S. aureus*, ATCC 25923), *Staphylococcus epidermidis* (*S. epidermidis*, ATCC 12228), and standard 3T3 mouse fibroblast cells were purchased from American Type Culture Collection (ATCC, Manassas, VA). Fresh whole blood of Wistar Hannover rat was purchased from InVivos Pte Ltd. (Singapore). The LIVE/DEAD BacLight Bacterial Viability Kit (containing SYTO 9 and propidium iodide), phalloidin, and 4',6-diamidino-2-phenylindole (DAPI) were purchased from Thermo Fisher (Waltham, MA).

2.2. Conjugation of antimicrobial peptide to the C-6 (hydroxyl) position of chitosan

6-Maleimidohexanoyl chloride (MICl) was prepared according to procedures reported in the literature with some modification.[30,31] MIAc (1056 mg, 5 mmol) was dissolved in 15 mL of dichloromethane, and 20 μL (1 drop) of dimethylformamide was added. The solution was cooled down to 0 °C in an ice bath and maintained under vigorous

stirring. The flask was vented with calcium chloride packing. Oxalyl chloride (762 mg, 6 mmol) was added dropwise to the solution for 15 min. After the addition, the reaction was allowed to proceed at room temperature for 3 h. The solvent was removed using rotary evaporator and dried under reduced pressure to obtain MICl (dark yellow solid, yield 95%).

CS (645 mg, 4 mmol saccharide unit) was dissolved in 20 mL of methanesulfonic acid under vigorous stirring. MICl (459 mg, 2 mmol) was dissolved in 4 mL methanesulfonic acid, and was added dropwise to the CS solution. The reaction was allowed to proceed overnight at room temperature. The solution was precipitated and washed in excess acetone, dialyzed against deionized water for 3 days (molecular weight cut-off, MWCO 3.5 kDa), and lyophilized to obtain maleimido-O-functionalized chitosan (CSOMI, brownish fluffy solid, yield 76%).

CSOMI (103 mg, 0.2 mmol maleimido moieties) was dissolved in 1 mL of PBS at pH 7.4. The solution was stirred and degassed with purified argon for 30 min. CysHHC10 (309 mg, 0.2 mmol) was added to the solution and the vial was quickly sealed. The solution was stirred at room temperature for 24 h. After reaction, the solution was dialyzed against deionized water for 3 days (MWCO 3.5 kDa) and lyophilized to obtain peptide-functionalized chitosan (CSOHHC, pale-yellow fluffy solid, yield 57%).

2.3. Conjugation of antimicrobial peptide to the C-2 (amino) position of chitosan

CS (1289 mg, 8 mmol saccharide unit) was dissolved in 50 mL of aqueous HCl solution 0.3 M. MIAc (845 mg, 4 mmol), EDC (745 mg, 4.8 mmol), and NHS (552 mg, 4.8 mmol) were dissolved in 20 mL of dimethyl sulfoxide, stirred for 30 min, and

added dropwise to the CS solution under vigorous stirring. The reaction was allowed to proceed at room temperature for 24 h. The mixture was dialyzed against deionized water for 3 days (MWCO 3.5 kDa) to obtain aqueous solution of maleimido-N-functionalized chitosan (CSNMI). The concentration of CSNMI solution was determined after lyophilizing small amount of the solution (yield 65%).

Aqueous CSNMI solution (52 mg CSNMI, 0.1 mmol maleimido moieties) was mixed with 2 mL of PBS at pH 7.4. The solution was stirred and degassed with purified argon for 30 min. CysHHC10 (155 mg, 0.1 mmol) was added to the solution and the vial was quickly sealed. The solution was stirred at room temperature for 24 h. After reaction, the solution was dialyzed against deionized water for 3 days (MWCO 3.5 kDa) and lyophilized to obtain peptide-functionalized chitosan (CSNHHC, white cotton-like solid, yield 55%).

2.4. Deposition of peptidopolysaccharides on SS substrates by TA-mediated layer-by-layer (LbL) assembly

The SS foils were cut into 1 cm × 1 cm coupons, cleaned with piranha solution, washed and dried according to the previous procedure.[32] TA solution (2 mg/mL) was prepared by dissolving TA in deionized water at pH 8.5 (adjusted with NaOH 2 M). Peptide-grafted CS solutions (2 mg/mL) were prepared by dissolving CSNHHC or CSOHHC in deionized water. The clean SS coupons were immersed alternatingly in the TA solution and peptide-grafted CS solution for 1 h each. The SS functionalized with TA (SS-TA) and SS functionalized with n-bilayers of TA and peptide-grafted CS (SS-CSNHHC$_n$ or SS-CSOHHC$_n$) substrates were immersed in deionized water for 1 h to remove any loosely-adhered compound and gently blown-dried with purified argon.

2.5. Characterization

Chemical structures of the compounds in deuterated water, dimethylsulfoxide, or chloroform were characterized by ^{1}H NMR spectroscopy on a Bruker ARX 500 MHz spectrometer. Size-exclusion gel permeation chromatography (GPC) was performed on a Waters GPC system equipped with a Waters 1515 isocratic HPLC pump, a Waters 717 plus autosampler injector, a Waters 2414 refractive index detector, and an Agilent PL aquagel-OH mixed-H 8 μm column, using aqueous sodium sulfate 0.05 M eluent at 35^{o}C and a flow rate of 1 mL/min. Zeta potential of the compounds in PBS at pH 7.4 and 22^{o}C was measured on a Malvern zetasizer. Surface compositions of the modified SS substrates were determined by X-ray photoelectron spectroscopy (XPS) on a Kratos AXIS Ultra DLD spectrometer, equipped with a monochromatized Al Kα X-ray source of 1486.71 eV photons with a constant dwell time of 100 ms, a pass energy of 40 eV, and a photoelectron take-off angle (α) of 90° with respect to the sample surface. Thickness of the bilayer coatings were determined using a VASE J.A. Woollam variable angle spectroscopic ellipsometer. Cross-sectional images of modified SS substrates were observed using a JEOL JSM-6700 field-emission scanning electron microscopy (FESEM). Bacteria and cell adhesions on the substrates were observed under a Nikon ECLIPSE T*i*-U fluorescence microscope.

2.6. Antimicrobial assays of the peptidopolysaccharides and peptidopolysaccharide-functionalized SS substrates

Bacterial cells were cultured to a mid-log phase in the respective growth media at 37°C according to ATCC protocols, and diluted to 2 × 10^{5} colony forming units (CFU)/mL in Mueller-Hinton broth (MHB). Stock solutions of sample compounds were prepared in MHB at a concentration of 2048 μg/mL, serially diluted by 2-fold,

and 100 μL of each dilution was placed in a 96-well plate (Greiner Bio-one, Germany). Then, 100 μL of bacterial suspension was added to each compound solution. The plate was incubated at 37°C overnight and observed by naked eye. Bacterial growth made the suspension appear cloudy, while the suspension with no bacterial growth remained clear.[33] The lowest concentration of the compound that inhibited the growth of bacteria was recorded as minimum inhibitory concentration (MIC). Subsequently, 100 μL of the suspension in the wells with no visible growth was spread on a Mueller-Hinton agar and incubated at 37°C overnight to observe the viability of the bacteria. The lowest concentration of the compound that killed 99.9% of the initially inoculated bacteria was recorded as minimum bactericidal concentration (MBC).

Mid-log phase bacterial cultures were washed and resuspended in PBS at a concentration of 10^7 cells/mL. The pristine and functionalized SS substrates were placed in a 24-well plate and immersed in 1 mL of the bacterial suspension at 37 °C for 4 h. After washing thrice with PBS to remove the loosely-adhered bacteria, each sample substrate was stained with LIVE/DEAD BacLight solution for 15 min and washed once with ultrapure water. The live (appearing green) and dead (appearing red) bacterial cells adhered on the sample surfaces were observed on a fluorescence microscope under a green filter (excitation/emission: 470 nm / 525 nm) and a red filter (excitation/emission: 535 nm / 645 nm).

2.7. Determination of hemolytic activity

Stock solutions of sample compounds were prepared in PBS at a concentration of 16384 μg/mL, serially diluted by 2-fold, and 100 μL of each dilution was placed in a 96-well plate. Fresh whole rat blood was dispersed in PBS at a concentration of 8%

(*v*/*v*), and 100 μL of the blood suspension was added to each compound solution. The blood suspension was added to blank PBS as negative control, and to PBS containing 0.1% (*v*/*v*) Triton X-100 as positive control. The plate was incubated at 37°C for 1 h to allow the interaction between the compounds and the blood cells. Each mixture was centrifuged at 1500 rpm for 10 min, and the optical absorbance of the supernatant was measured at 560 nm wavelength under a UV microplate reader (Multiskan GO, Thermo Scientific). The percentage of hemoglobin release was calculated as $[(A_S - A_N) / (A_P - A_N)] \times 100\%$, where A_S, A_N, and A_P are the optical absorbance of the supernatant from the incubated sample, negative control, and positive control, respectively.

2.7. Cytotoxicity assay

Metabolic MTT assay was carried out to determine the cytotoxicity of the sample compounds. 3T3 fibroblast cells were cultured and resuspended in Dulbecco's modified Eagle's medium (DMEM) supplemented with 10% fetal bovine serum, 1 mM L-glutamine, and 100 IU/mL penicillin. Then, 100 μL of the suspension containing 5000 cells were placed in each well of a 96-well plate. The plate was incubated in a humidified atmosphere of 95% air and 5% CO_2 at 37°C for 24 h. Sample solutions were prepared by dissolving the respective compounds in the supplemented DMEM at 2-fold serial dilutions. The medium in each well was replaced with 100 μL of the sample solutions, and the plate was incubated at 37°C for 24 h. Nontoxic control experiment was carried out using the supplemented DMEM without any compound. The medium in each well was then replaced with 100 μL of MTT solution (0.5 mg/mL of MTT concentration in supplemented DMEM). After additional incubation at 37°C for 4 h, the supernatant was aspirated and 100 μL of dimethyl sulfoxide was added to dissolve the internalized formazan crystal. After 15

min, the optical absorbance was measured at 600 nm wavelength using a UV microplate reader and expressed as a percentage relative to the absorbance of the nontoxic control.

Cytotoxicity of the modified substrates was determined using cells adhesion assay. The 3T3 fibroblasts were resuspended in supplemented DMEM at a concentration of 2×10^5 cells/mL. The pristine and modified SS substrates were placed in a 24-well plate and covered with 1 mL of cells suspension. The substrates were incubated at 37°C for 24 h and washed thrice with PBS. The adhered cells were fixated using 1 mL of PBS containing 4% (*v*/*v*) paraformaldehyde for 15 min and washed thrice with PBS. The fixated cells were treated with PBS containing 0.1% (*v*/*v*) Triton X-100 for 5 min and washed thrice with PBS. The treated cells were stained using 0.5 mL of PBS containing 1.5 μL of phalloidin and 1 μL of DAPI for 15 min, and washed thrice with PBS. The stained cells on the substrates were observed on a fluorescence microscope under a green filter (excitation/emission: 470 nm / 525 nm) and a blue filter (excitation/emission: 350 nm / 460 nm). The amount of adhered 3T3 fibroblast cells was counted using National Institute of Health (NIH) ImageJ software. Statistical analysis of the results over 3 fluorescence micrographs was performed under one-way analysis of variance (ANOVA) using a Tukey's post hoc test.

3. Results and Discussion

3.1. Preparation of the chitosan-based peptidopolysaccharides (Scheme 1)

The O-acylation of chitosan with acyl chloride to introduce maleimide functions was carried out by maintaining salt formation of the primary amino groups with a strong protonating solvent. In this amine-protected environment, the substitution site with acyl group occurred mainly at the C-6 position and less at the C-3 position.[29] To ensure major substitution at the C-6 position, the acyl chloride was set as the limiting reactant in the molar-feed composition. The ^{1}H NMR spectrum of the maleimido-O-functionalized chitosan (CSOMI, Figure 1) is predominated by the chemical shifts of glucosamine unit protons at 3.1, 3.5–4.1, and 4.8 ppm.[34] New chemical shifts at 1.3, 1.5, 2.0, and 3.3 ppm arise from the alkane protons of hexanoyl linker, indicating successful acetylation of chitosan.[35] The appearance of chemical shift at 6.8 ppm also signifies the presence of 'clickable' maleimido group on CSOMI. The conjugation of cationic peptide with chitosan was carried out via thiol-maleimide 'click' reaction between the cysteine unit of CysHHC10 and the maleimido groups of CSOMI. This reaction occurred spontaneously without catalytic assistance, thus avoiding any metal or organic residues which may interfere with the biological functions. Below pH 7.4, the maleimido group might also react with the nucleophilic amines of peptide, ensuring complete conjugation of the maleimide functions, albeit resulting in uncertainty of the final structure. The chemical shift characteristics of CSOMI and CysHHC10 appear concomitantly in the ^{1}H NMR spectrum of the HHC10-O-functionalized chitosan (CSOHHC), suggesting the presence of pendent peptide moieties grafted to the chitosan backbone (Figure 1).

The introduction of maleimide functions to the C-2 position of chitosan was carried out by N-amidation with succinimide-activated 6-maleimidohexanoic acid (MIAc) to

obtain the maleimido-N-functionalized chitosan (CSNMI) solution. Notably, the solid form of CSNMI was water insoluble, probably due to the lack of protonation ability of the secondary amines after amide formation. After dialysis, the aqueous CSNMI solution was subjected to thiol-maleimide 'click' reaction with CysHHC10 peptide to obtain the HHC10-N-functionalized chitosan (CSNHHC). The chemical shift characteristics of CS, maleimidohexanoic linker, and CysHHC10 appear concomitantly in the ^{1}H NMR spectrum of the CSNHHC peptidopolysaccharide (Figure 1), confirming the successful conjugation of pendent peptide moieties to the chitosan backbone. The solid form of CSNHHC was water soluble due to the protonation of the abundant primary amino groups in the grafted peptide.

In the 2D ^{1}H–^{13}C heteronuclear multiple bond correlation (HMBC) spectra of CSOMI and CSNMI (Figure S1 and S2, Supporting Information), the signal crowding at f_1 55–98 ppm were dominated by the correlations among chitosan signals, while most of the correlations among the hexanoic linker signals are present at f_1 22–38 ppm. In the CSOMI spectrum, the signal at f_1 174 ppm and f_2 2 ppm arose from the correlation between ester carbon and the adjacent proton of hexanoic linker, indicating the successful O-acylation. In the CSNMI spectrum, the signal at f_1 184 ppm and f_2 2 ppm emerged due to the correlation between amide carbon and the adjacent proton of hexanoic linker, indicating successful N-amidation. Because amide carbon exhibits higher shift than ester carbon, this evidence confirms the difference in molecular configuration between CSOMI and CSNMI. It is assumed that the O-acylation occurred mainly at the C-6 position and less at the C-3 position due to steric orientation, although the exact percentage cannot be concluded.[29]

In the ^{1}H NMR spectra of the peptidopolysaccharides (Figure 1), the chemical shift at 3.5 ppm is attributable to the methine proton in the C-5 position of the chitosan units, whereas that at 0.75 and 0.63 ppm are attributable to the methyl protons of the CysHHC10 units. Based on the integration of the peak areas of these chemical shifts, the mass fractions of the peptide unit in the CSNHHC and CSOHHC peptidopolysaccharides are calculated to be 45.2% and 47.6%, respectively (Table 1). The degree of substitution (DS) of CSOMI was slightly higher than that of CSNMI. Chitosan unit provides two sites (C-6 and C-3 positions) for O-acylation, as compared to only one site (C-2 position) for N-amidation. Upon the peptide conjugations, the DS for conjugated peptide decreased only slightly from the conjugated maleimide, implying high efficiency of the thiol-maleimide 'click' reaction. The zeta potential (ζ) values of the chitosan and maleimido-functionalized chitosans did not show appreciable difference, but increased significantly upon conjugation with the cationic peptide, implying the superior electrophoretic mobility of peptidopolysaccharides due to the presence of positive charges on the molecules.

From the size-exclusion gel permeation chromatography (GPC), the number-average molecular weight (M_n) and polydispersity (M_w/M_n) of the chitosan-based compounds increased progressively with the conjugations of maleimide linkers and CysHHC10 peptide (Figure S3), in agreement with the increasing size and complexity of the macromolecules. According to the M_n data, the pristine chitosan consists of 119 repeat units. Previously, M_n determination of chitosan compounds has been reported using PL aquagel-OH mixed (300 mm) column, aqueous acetic acid/sodium acetate eluent, and non-charged poly(ethylene oxide)/poly(ethylene glycol) standards of 1970–1345000 g/mol.[36] In the present work, similar type of column and standards were

used, and aqueous sodium sulfate eluent was employed to minimize the interaction between the charged polymers and the column. The use of non-charged standards and vinyl-based stationary phase to characterize charged polymers imposed a limitation in the M_n determination. It should be noted that GPC data show estimates of relative M_n and might not reflect the actual values, because correct determination of M_n for these polymers was challenging due to structural variation accompanied by differences in hydrodynamic size, shape, and refractive index increment (dn/dc ratio).

3.2. Preparation of the peptidopolysaccharide coatings via polyphenol-mediated chemistry (Scheme 1)

The antibacterial coatings can be constructed via layer-by-layer (LbL) assembly of tannic acid (TA) and peptidopolysaccharides. The polyphenolic groups of TA readily chelate the metal centre of stainless steel (SS) substrates by the formation of tridentate coordination complexes.[37] In comparison of the XPS wide-scan spectra (Figures 2a and 2b) of the SS and TA-anchored SS surface (SS-TA), the increase in intensity of C 1s core-level signal in the latter is consistent with the presence of an organic TA layer on the SS substrate. The disappearance of characteristic signals of SS metal viz., Cr $2p_{3/2}$, Fe $2p_{3/2}$ and Ni $2p_{3/2}$ core-level components with respective binding energies (BEs) at 577, 711 and 860 eV, suggests that the thickness of TA layer had exceeded the ~8 nm probing depth in organic matrices of the XPS technique.[38] The abundant trihydroxyphenyl sites on the SS-TA surfaces can readily bind with the amino moieties of the peptidopolysaccharides through Michael addition or Schiff base reaction.[39] A new N 1s core-level signal has emerged in the SS-CSNHHC$_n$ and SS-CSOHHC$_n$ surfaces (Figure 2c–f), confirming the incorporation of peptidopolysaccharides in the multilayer coatings. The intensity of N 1s signal also increases with the increase in number of the peptidopolysaccharide layer. From the

cross-sectional view of field-emission scanning electron microscopy (FESEM) images (Figure 3a–c), the coating thicknesses of the bilayers on SS-CSNHHC$_{10}$ and SS-CSOHHC$_{10}$ surfaces have reached 270 and 400 nm, respectively. The coating thickness also increases approximately linearly with the number of bilayers (Figure 3d).

3.3. Antimicrobial activities of the chitosan-based peptidopolysaccharides

The antimicrobial properties of the peptidopolysaccharides towards Gram-negative (*Escherichia coli* and *Pseudomonas aeruginosa*) and Gram-positive (*Staphylococcus aureus* and *epidermidis*) bacteria were investigated based on their minimum inhibitory concentration (MIC) using the broth dilution method. Polymers that do not contain AMP, namely CS and CSOMI, did not show any activity towards all the bacteria challenged up to the highest concentration tested (Table 2). On the contrary, the native CysHHC10 peptide exhibited strong antimicrobial activity in the MIC range of 8 to 64 μg/mL towards all bacteria. In comparison to that of native AMP, the MIC values of CSNHHC peptidopolysaccharides increased by several-fold towards all bacteria. The increase in MIC values was due to the inclusion of chitosan moiety, implying that the antimicrobial effect was mainly contributed by the AMP content in the peptidopolysaccharide molecules. It has also been reported that non-bactericidal CS backbone contributed to overall mass of nisin-conjugated CS, resulting in lower antimicrobial potency towards *E. coli* and *S. aureus* as compared to free nisin.[24] Interestingly, compared to the native AMP, CSOHHC showed similar MIC values towards Gram-positive bacteria, and only two-fold increase of MIC values towards Gram-negative bacteria. On the basis of peptide mass fraction, CSOHHC exhibited MIC values lower than that of the native AMP, namely at 15 and 4 μg/mL (in comparison to the corresponding values of 32 and 8 μg/mL) towards *S. aureus* and

epidermidis, respectively. In general, the outermost surface of Gram-positive bacteria is encased with a thick peptidoglycan layer, whereas the cell wall of Gram-negative bacteria mainly consists of lipid bilayer. Due to the resemblance of CSOHHC with the peptidoglycan structure, it is postulated that the peptidopolysaccharide exhibited affinity and infiltration capability towards the cell wall of Gram-positive bacteria, leading to the improved inhibitory of growth. The antimicrobial activity of CSOHHC was found to be higher than that of CSNHHC, presumably due to the free amino group on the peptidopolysaccharide backbone which increased the protonation capacity and water solubility. It was also reported that primary amine could exist in an equilibrium form between free amine (no charge) and protonated amine (positively charged), and its antibacterial effect decreased upon introduction of more alkyl arms or rigid structure.[40] The CSOHHC retained a higher DS than CSNHHC, and thus also exhibited higher antimicrobial activity due to higher peptide content. The influence of DS on activity has been reported and reviewed.[41] It has also been reported that the arginine-functionalized chitosan with higher DS was more effective in permeabilizing the cell membrane of *E. coli* and *P. fluorescens* than the same derivative with lower DS.[42] The parameter of killing efficacy is expressed as minimum bactericidal concentration (MBC, Table S1), which were consistently recorded twice the MIC values as an indication to the potency of peptidopolysaccharides to eradicate pathogens.

3.5. Hemotoxicity and cytotoxicity of the chitosan-based peptidopolysaccharides

Hemotoxicity and cytotoxicity of the peptidopolysaccharides were assayed with rat whole blood and mouse 3T3 fibroblast cells, respectively, as the model mammalian standards. The hemolytic parameter was determined by measuring the lowest concentration of a compound which incites lysis towards 50% of the red blood cells

(HC_{50}). The half maximal inhibitory concentration (IC_{50}) of a compound was determined by measuring the metabolic methylthiazolyldiphenyl-tetrazolium bromide (MTT) residue to express its cytotoxicity. The compounds with no AMP content, namely CS and CSOMI, did not show any hemolytic activity up to the highest concentration tested at 16384 μg/mL (Table 2). Similarly, they did not show any indication of cytotoxicity up to the highest concentration tested at 2048 μg/mL. The CysHHC10 peptide exhibited strong hemo- and cytotoxicity with HC_{50} and IC_{50} values of 1024 and 84 μg/mL, respectively. Upon conjugation to chitosan backbone, the HC_{50} and IC_{50} values of the CSNHHC and CSOHHC peptidopolysaccharides increased several folds in comparison to that of the CysHHC10 peptide. In addition, at any effective concentration, the cell viability of fibroblasts incubated with the peptidopolysaccharides was higher than that incubated with CysHHC10 (Figure 4). These results indicate that the biocompatible nature of the chitosan backbone can be molecularly engineered to moderate the toxicity of AMP.

Therapeutic indices of the antimicrobial compounds were expressed by measuring the quantitative ratio between biocompatibility and efficacy to obtain the hemoselectivity (HC_{50}/MIC) and cytoselectivity (IC_{50}/MIC) values (Table 2). The hemoselectivity of CysHHC10 is higher than other AMPs, for example indolicidin,[43] melittin,[44] magainin and protegrin[45] with HC_{50}/MIC (towards *S. aureus*) values of 8, 8, 5 and 3, respectively. In general, the CSNHHC and CSOHHC peptidopolysaccharides exhibited HC_{50}/MIC values higher than that of the CysHHC10, implying that conjugation with the chitosan backbone have increased the hemoselectivity of the native AMP. In comparison to the CysHHC10 peptide, the CSOHHC peptidopolysaccharides exhibited four- and two-fold increases in HC_{50}/MIC and

IC_{50}/MIC values, respectively, when calculated using MIC towards both *Staphylococci*. The structural mimetic of peptidoglycan in CSOHHC presumably has contributed to its selective targeting of the Gram-positive bacterial membranes, leading to the improved therapeutic indices.

3.6. Antibacterial activity and cytocompatibility of the peptidopolysaccharide-functionalized surfaces

Antibacterial coatings consisting of the chitosan-based peptidopolysaccharides and tannic acid (TA) were constructed on stainless steel (SS) surface via layer-by-layer assembly. After being immersed in the bacterial suspension (10^7 cells/mL) for 4 h, the pristine SS and TA-functionalized SS (SS-TA) surfaces were colonized by live (appearing green) *E. coli* and *S. aureus*, indicating their susceptibility towards bacterial adhesion (Figure 5). On the contrary, most of the bacteria adhered on the TA-peptidopolysaccharide functionalized SS (SS-CSNHHC$_{10}$ and SS-CSOHHC$_{10}$) surfaces were compromised (appearing red), confirming the antibacterial properties of the peptidopolysaccharide coatings. The cationic peptidopolysaccharide layers presumably have instigated membrane permeability and destabilization upon contact, leading to the death of Gram-negative and -positive bacteria. Surface cytocompatibility is also of an equally important criterion in biomaterial applications. Mouse fibroblasts (2×10^5 cells/mL) were incubated with the pristine and functionalized SS surfaces, followed by the nucleic and cytoplasmic staining with 4',6-diamidino-2-phenylindole (DAPI) and phalloidin. A large number of viable cells were able to adhere and proliferate on the nontoxic SS surface, while a smaller number of viable cells adhered on the peptidopolysaccharide-functionalized SS surfaces (Figure 6). The viability of adhered cells on the SS-CSNHHC$_{10}$ and SS-CSOHHC$_{10}$ surfaces were 66 and 62%, respectively, relative to that of the SS surface.

These results demonstrated potential applications of the peptidopolysaccharides as antibacterial coatings with moderate cytocompatible properties.

4. Conclusion

Peptidopolysaccharides with peptidoglycan-mimetic structures were prepared by grafting CysHHC10 peptide to the C-2 (amino) or C-6 (hydroxyl) position of the chitosan backbone via thiol-maleimide 'click' conjugation, utilizing the maleimidohexanoic linkers. The peptidopolysaccharide with primary amino backbone intact (CSOHHC) showed higher bactericidal activity as compared to that with the amino backbone grafted with the peptide (CSNHHC). The CSOHHC peptidopolysaccharide increased the hemo- and cytoselectivity of the free peptide towards *Staphylococci* by four- and two-fold, respectively, consistent with its peptidoglycan-mimetic structure for targeting the Gram-positive bacteria. This improved therapeutic index indicates the successful molecular engineering approach to moderating the toxicity of AMP without losing its activity. Antibacterial coatings consisting of peptidopolysaccharide and tannic acid layers could be constructed via layer-by-layer assembly, to give rise to peptidopolysaccharides-based antimicrobial surfaces. In the static adhesion assay, *E. coli* and *S. aureus* adhered on the peptidopolysaccharide coatings were killed upon contact. On the other hand, the adhered 3T3 cells retained more than 60% viability on the peptidopolysaccharide coatings. The antibacterial efficacy and cytocompatibility of the present peptidopolysaccharides and coatings thus readily suggest their applicability in biomedical and healthcare fields.

Associated Content

The Supporting Information is available free of charge on the ACS Publications website.

MBC values, $^{1}H–^{13}C$ HMBC spectra, GPC chromatograms of the chitosan derivatives and peptidopolysaccharides, XPS spectra and surface elemental stoichiometries of the peptidopolysaccharide coatings, detailed ^{1}H NMR spectra of all compounds, and determinations of DS, yields, and surface coatings density.

Acknowledgement

This work was funded and supported by a Singapore Ministry of Education Tier 3 Grant (MOE2013-T3-1-002).

References

1. Cansizoglu, M. F.; Toprak, E. Fighting against evolution of antibiotic resistance by utilizing evolvable antimicrobial drugs. *Curr. Genet.* **2017**, *63*, 973-976.
2. Pu, Y.; Hou, Z.; Khin, M. M.; Zamudio-Vázquez, R.; Poon, K. L.; Duan, H.; Chan-Park, M. B. Synthesis and antibacterial study of sulfobetaine/quaternary ammonium-modified star-shaped poly[2-(dimethylamino)ethyl methacrylate]-based copolymers with an inorganic core. *Biomacromolecules* **2017**, *18*, 44-55.
3. Locock, K. E. S.; Michl, T. D.; Stevens, N.; Hayball, J. D.; Vasilev, K.; Postma, A.; Griesser, H. J.; Meagher, L.; Haeussler, M. Antimicrobial polymethacrylates synthesized as mimics of tryptophan-rich cationic peptides. *ACS Macro Lett.* **2014**, *3*, 319-323.
4. Venkataraman, S.; Tan, J. P. K.; Ng, V. W. L.; Tan, E. W. P.; Hedrick, J. L.; Yang, Y. Y. Amphiphilic and hydrophilic block copolymers from aliphatic N-substituted 8-membered cyclic carbonates: A versatile macromolecular platform for biomedical applications. *Biomacromolecules* **2017**, *18*, 178-188.
5. Yang, C.; Krishnamurthy, S.; Liu, J.; Liu, S.; Lu, X.; Coady, D. J.; Cheng, W.; De Libero, G.; Singhal, A.; Hedrick, J. L.; Yang, Y. Y. Broad-spectrum antimicrobial star polycarbonates functionalized with mannose for targeting bacteria residing inside immune cells. *Adv. Healthc. Mater.* **2016**, *5*, 1272-1281.
6. Nimmagadda, A.; Liu, X.; Teng, P.; Su, M.; Li, Y.; Qiao, Q.; Khadka, N. K.; Sun, X.; Pan, J.; Xu, H.; Li, Q.; Cai, J. Polycarbonates with potent and selective antimicrobial activity toward Gram-positive bacteria. *Biomacromolecules* **2017**, *18*, 87-95.
7. Liu, R.; Chen, X.; Falk, S. P.; Masters, K. S.; Weisblum, B.; Gellman, S. H. Nylon-3 polymers active against drug-resistant *Candida albicans* biofilms. *J. Am. Chem. Soc.* **2015**, *137*, 2183-2186.
8. Liu, R.; Suárez, J. M.; Weisblum, B.; Gellman, S. H.; McBride, S. M. Synthetic polymers active against *Clostridium difficile* vegetative cell growth and spore outgrowth. *J. Am. Chem. Soc.* **2014**, *136*, 14498-14504.
9. Stratton, T. R.; Applegate, B. M.; Youngblood, J. P. Effect of steric hindrance on the properties of antibacterial and biocompatible copolymers. *Biomacromolecules* **2011**, *12*, 50-56.
10. Lienkamp, K.; Madkour, A. E.; Musante, A.; Nelson, C. F.; Nüsslein, K.; Tew, G. N. Antimicrobial polymers prepared by ROMP with unprecedented selectivity: A molecular construction kit approach. *J. Am. Chem. Soc.* **2008**, *130*, 9836-9843.
11. Ilker, M. F.; Nüsslein, K.; Tew, G. N.; Coughlin, E. B. Tuning the hemolytic and antibacterial activities of amphiphilic polynorbornene derivatives. *J. Am. Chem. Soc.* **2004**, *126*, 15870-15875.
12. Gao, Q.; Li, P.; Zhao, H.; Chen, Y.; Jiang, L.; Ma, P. X. Methacrylate-ended polypeptides and polypeptoids for antimicrobial and antifouling coatings. *Polym. Chem.* **2017**, *8*, 6386-6397.
13. Chongsiriwatana, N. P.; Patch, J. A.; Czyzewski, A. M.; Dohm, M. T.; Ivankin, A.; Gidalevitz, D.; Zuckermann, R. N.; Barron, A. E. Peptoids that mimic the

structure, function, and mechanism of helical antimicrobial peptides. *Proc. Natl. Acad. Sci.* **2008**, *105*, 2794-2799.

14. Hancock, R. E. W.; Sahl, H.-G. Antimicrobial and host-defense peptides as new anti-infective therapeutic strategies. *Nat. Biotechnol.* **2006**, *24*, 1551-1557.
15. Morris, C. J.; Beck, K.; Fox, M. A.; Ulaeto, D.; Clark, G. C.; Gumbleton, M. PEGylation of antimicrobial peptides maintains the active peptide conformation, model membrane interactions, and antimicrobial activity while improving lung tissue biocompatibility following airway delivery. *Antimicrob. Agents Chemother.* **2012**, *56*, 3298-3308.
16. Lee, W.; Park, E. J.; Min, G.; Choi, J.; Na, D. H.; Bae, J. S. Dual functioned pegylated phospholipid micelles containing cationic antimicrobial decapeptide for treating sepsis. *Theranostics* **2017**, *7*, 3759-3767.
17. Kumar, P.; Takayesu, A.; Abbasi, U.; Kalathottukaren, M. T.; Abbina, S.; Kizhakkedathu, J. N.; Straus, S. K. Antimicrobial peptide–polymer conjugates with high activity: Influence of polymer molecular weight and peptide sequence on antimicrobial activity, proteolysis, and biocompatibility. *ACS Appl. Mater. Interfaces* **2017**, *9*, 37575-37586.
18. Kumar, P.; Shenoi, R. A.; Lai, B. F. L.; Nguyen, M.; Kizhakkedathu, J. N.; Straus, S. K. Conjugation of aurein 2.2 to HPG yields an antimicrobial with better properties. *Biomacromolecules* **2015**, *16*, 913-923.
19. Pranantyo, D.; Xu, L. Q.; Hou, Z.; Kang, E.-T.; Chan-Park, M. B. Increasing bacterial affinity and cytocompatibility with four-arm star glycopolymers and antimicrobial α-polylysine. *Polym. Chem.* **2017**, *8*, 3364-3373.
20. He, M.; Wang, X.; Wang, Z.; Chen, L.; Lu, Y.; Zhang, X.; Li, M.; Liu, Z.; Zhang, Y.; Xia, H.; Zhang, L. Biocompatible and biodegradable bioplastics constructed from chitin via a "green" pathway for bone repair. *ACS Sustain. Chem. Eng.* **2017**, *5*, 9126-9135.
21. Li, P.; Zhou, C.; Rayatpisheh, S.; Ye, K.; Poon, Y. F.; Hammond, P. T.; Duan, H.; Chan-Park, M. B. Cationic peptidopolysaccharides show excellent broad-spectrum antimicrobial activities and high selectivity. *Adv. Mater.* **2012**, *24*, 4130-4137.
22. Su, Y.; Tian, L.; Yu, M.; Gao, Q.; Wang, D.; Xi, Y.; Yang, P.; Lei, B.; Ma, P. X.; Li, P. Cationic peptidopolysaccharides synthesized by 'click' chemistry with enhanced broad-spectrum antimicrobial activities. *Polym. Chem.* **2017**, *8*, 3788-3800.
23. Qi, G.-B.; Zhang, D.; Liu, F.-H.; Qiao, Z.-Y.; Wang, H. An "on-site transformation" strategy for treatment of bacterial infection. *Adv. Mater.* **2017**, *29*, 1703461-n/a.
24. Min, L.; Liu, M.; Zhu, C.; Liu, L.; Rao, Z.; Fan, L. Synthesis and in vitro antimicrobial and antioxidant activities of quaternary ammonium chitosan modified with nisin. *J. Biomater. Sci. Polym. Ed.* **2017**, *28*, 2034-2052.
25. Sahariah, P.; Sorensen, K. K.; Hjalmarsdottir, M. A.; Sigurjonsson, O. E.; Jensen, K. J.; Masson, M.; Thygesen, M. B. Antimicrobial peptide shows enhanced activity and reduced toxicity upon grafting to chitosan polymers. *Chem. Commun.* **2015**, *51*, 11611-11614.

26. Cherkasov, A.; Hilpert, K.; Jenssen, H.; Fjell, C. D.; Waldbrook, M.; Mullaly, S. C.; Volkmer, R.; Hancock, R. E. W. Use of artificial intelligence in the design of small peptide antibiotics effective against a broad spectrum of highly antibiotic-resistant superbugs. *ACS Chem. Biol.* **2009**, *4*, 65-74.

27. Hancock, R. E. W.; Hilpert, K.; Cherkasov, A.; Fjell, C.; Google Patents: 2008.

28. Pranantyo, D.; Xu, L. Q.; Kang, E.-T.; Mya, M. K.; Chan-Park, M. B. Conjugation of polyphosphoester and antimicrobial peptide for enhanced bactericidal activity and biocompatibility. *Biomacromolecules* **2016**, *17*, 4037-4044.

29. Sashiwa, H.; Kawasaki, N.; Nakayama, A.; Muraki, E.; Yamamoto, N.; Zhu, H.; Nagano, H.; Omura, Y.; Saimoto, H.; Shigemasa, Y.; Aiba, S.-i. Chemical modification of chitosan. 13. Synthesis of organosoluble, palladium adsorbable, and biodegradable chitosan derivatives toward the chemical plating on plastics. *Biomacromolecules* **2002**, *3*, 1120-1125.

30. Filice, M.; Romero, O.; Guisan, J. M.; Palomo, J. M. trans,trans-2,4-Hexadiene incorporation on enzymes for site-specific immobilization and fluorescent labeling. *Org. Biomol. Chem.* **2011**, *9*, 5535-5540.

31. Duval, A.; Lange, H.; Lawoko, M.; Crestini, C. Reversible crosslinking of lignin via the furan-maleimide Diels-Alder reaction. *Green Chem.* **2015**, *17*, 4991-5000.

32. Xu, L. Q.; Pranantyo, D.; Neoh, K.-G.; Kang, E.-T.; Teo, S. L.-M.; Fu, G. D. Synthesis of catechol and zwitterion-bifunctionalized poly(ethylene glycol) for the construction of antifouling surfaces. *Polym. Chem.* **2016**.

33. Wikler, M. A. *Methods for dilution antimicrobial susceptibility tests for bacteria that grow aerobically: Approved standard*; Clinical Laboratory Standards Institute: Pennsylvania, 2009.

34. Belabassi, Y.; Moreau, J.; Gheran, V.; Henoumont, C.; Robert, A.; Callewaert, M.; Rigaux, G.; Cadiou, C.; Vander Elst, L.; Laurent, S.; Muller, R. N.; Dinischiotu, A.; Voicu, S. N.; Chuburu, F. Synthesis and characterization of PEGylated and fluorinated chitosans: Application to the synthesis of targeted nanoparticles for drug delivery. *Biomacromolecules* **2017**, *18*, 2756-2766.

35. Zhao, D.; Zhang, H.; Tao, W.; Wei, W.; Sun, J.; He, Z. A rapid albumin-binding 5-fluorouracil prodrug with a prolonged circulation time and enhanced antitumor activity. *Biomater. Sci.* **2017**, *5*, 502-510.

36. Zielinska, K.; Shostenko, A. G.; Truszkowski, S. Analysis of chitosan by gel permeation chromatography. *High Energ. Chem.* **2014**, *48*, 72-75.

37. Pranantyo, D.; Xu, L. Q.; Neoh, K.-G.; Kang, E.-T.; Ng, Y. X.; Teo, S. L.-M. Tea stains-inspired initiator primer for surface grafting of antifouling and antimicrobial polymer brush coatings. *Biomacromolecules* **2015**, *16*, 723-732.

38. Pranantyo, D.; Xu, L. Q.; Neoh, K. G.; Kang, E.-T.; Teo, S. L.-M. Antifouling coatings via tethering of hyperbranched polyglycerols on biomimetic anchors. *Ind. Eng. Chem. Res.* **2016**, *55*, 1890-1901.

39. Xu, G.; Pranantyo, D.; Zhang, B.; Xu, L.; Neoh, K.-G.; Kang, E.-T. Tannic acid anchored layer-by-layer covalent deposition of parasin I peptide for antifouling and antimicrobial coatings. *RSC Advances* **2016**, *6*, 14809-14818.

40. Palermo, E. F.; Kuroda, K. Chemical structure of cationic groups in amphiphilic polymethacrylates modulates the antimicrobial and hemolytic activities. *Biomacromolecules* **2009**, *10*, 1416-1428.

41. Sahariah, P.; Másson, M. Antimicrobial chitosan and chitosan derivatives: A review of the structure–activity relationship. *Biomacromolecules* **2017**, *18*, 3846-3868.

42. Tang, H.; Zhang, P.; Kieft, T. L.; Ryan, S. J.; Baker, S. M.; Wiesmann, W. P.; Rogelj, S. Antibacterial action of a novel functionalized chitosan-arginine against Gram-negative bacteria. *Acta Biomaterialia* **2010**, *6*, 2562-2571.

43. Jindal, H. M.; Le, C. F.; Mohd Yusof, M. Y.; Velayuthan, R. D.; Lee, V. S.; Zain, S. M.; Isa, D. M.; Sekaran, S. D. Antimicrobial activity of novel synthetic peptides derived from indolicidin and ranalexin against *Streptococcus pneumoniae*. *PLoS One* **2015**, *10*, e0128532.

44. Zhu, W. L.; Nan, Y. H.; Hahm, K. S.; Shin, S. Y. Cell selectivity of an antimicrobial peptide melittin diastereomer with D-amino acid in the leucine zipper sequence. *J. Biochem. Mol. Biol.* **2007**, *40*, 1090-1094.

45. Rotem, S.; Radzishevsky, I.; Mor, A. Physicochemical properties that enhance discriminative antibacterial activity of short dermaseptin derivatives. *Antimicrob. Agents Chemother.* **2006**, *50*, 2666-2672.

Captions for Scheme, Tables and Figures

Scheme 1. Preparation of the peptidopolysaccharides by conjugation of AMP to the C-2 (amine) or C-6 (hydroxyl) positions of chitosan, and peptidopolysaccharide functionalization of SS substrates via LbL assembly mediated by tannic acid.

Table 1. Molecular weight, zeta potential, and composition of the polysaccharides and peptidopolysaccharide conjugates.

Table 2. Antimicrobial activity, hemolytic effect, cytotoxicity and therapeutic index of the polysaccharides and peptidopolysaccharide conjugates.

Figure 1. ^{1}H NMR spectra of the polysaccharides and peptidopolysaccharide conjugates.

Figure 2. XPS wide-scan spectra of the (a) pristine SS, (b) TA-modified SS, and (c–f) SS surfaces coated with 5- and 10-bilayers of TA and peptidopolysaccharides.

Figure 3. Cross-sectional FESEM images of the (a) pristine SS, (b) SS-$CSNHC_{10}$, (c) SS-$CSOHHC_{10}$ surfaces, and (d) coating thickness of the TA-peptidopolysaccharide bilayers on SS surfaces measured using ellipsometry. Scale bar is 100 nm. Error bar denotes standard deviation obtained from three replicates.

Figure 4. Relative cell viability of the 3T3 fibroblasts after 24-h incubation with the polysaccharides and peptidopolysaccharide conjugates. Error bar denotes standard deviation obtained from three replicates.

Figure 5. Fluorescence micrographs of live (green) and dead (red) *E. coli* (a–d) and *S. aureus* (e–h) adhered to the (a,e) pristine SS, (b,f) SS-TA, (c,g) SS-CSNHHC$_{10}$, and (d,h) SS-CSOHHC$_{10}$ surfaces after 4-h immersion in the bacterial suspension (10^7 cells/mL) at 37 °C. Scale bar is 50 μm.

Figure 6. Fluorescence micrographs of 3T3 fibroblasts adhered to the (a) pristine SS, (b) SS-CSNHHC$_{10}$, and (c) SS-CSOHHC$_{10}$ surfaces after 24-h immersion in the cells suspension (2×10^5 cells/mL) at 37 °C and (d) their relative count of cell viability. Scale bar is 200 μm. Error bar denotes standard deviation obtained from three replicates. Asterisk (*) denotes significant difference with p-value < 0.05 (Tukey's test).

Scheme 1.

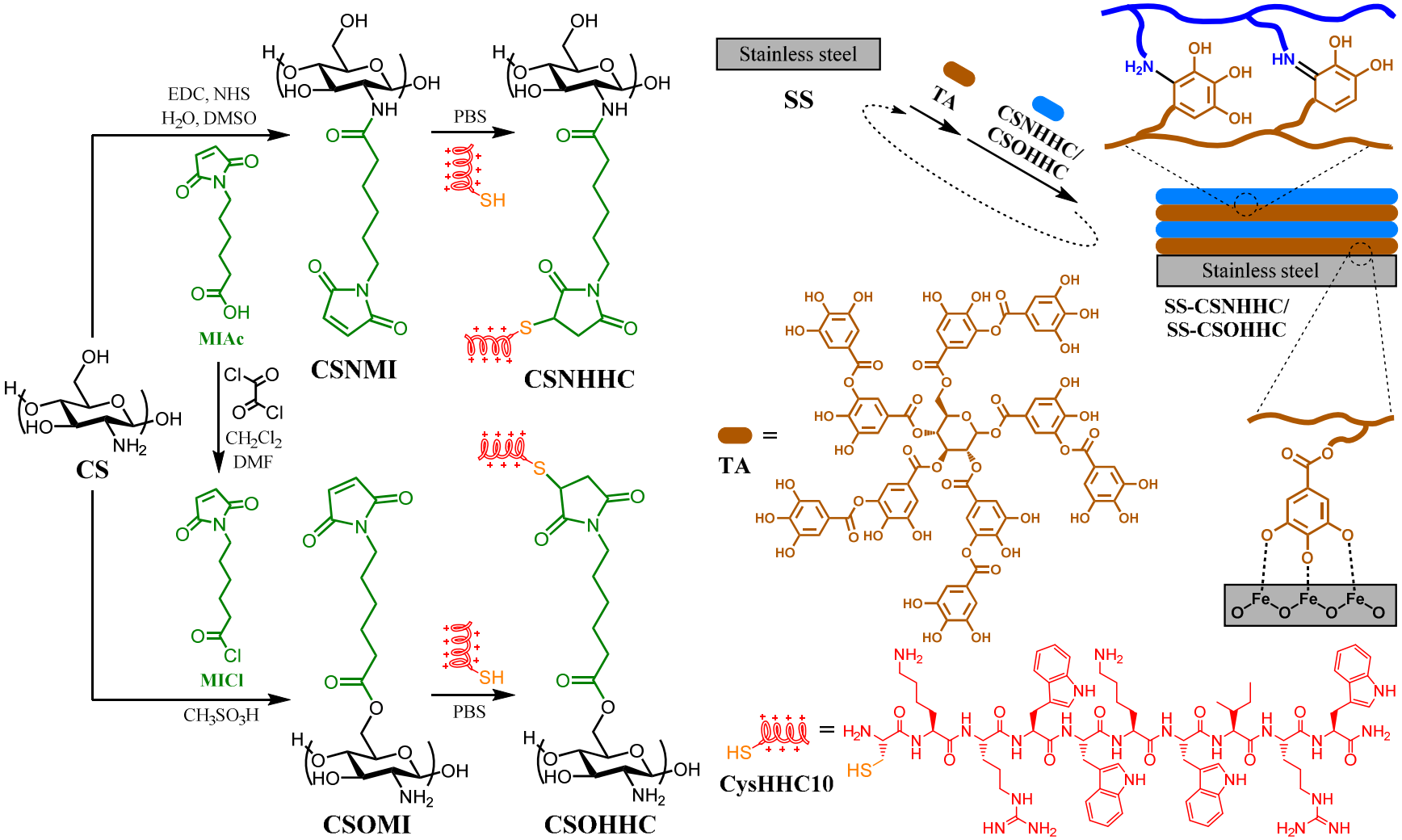
EDC, NHS
H2O, DMSO
MIAc
CSNMI
PBS
CSNHHC
CS
CH2Cl2
DMF
MICl
CH3SO3H
CSOMI
PBS
CSOHHC
Stainless steel
SS
TA
CSNHHC/
CSOHHC
Stainless steel
SS-CSNHHC/
SS-CSOHHC
TA
CysHHC10

Table 1. Molecular weight, zeta potential, and composition of the polysaccharides and peptidopolysaccharide conjugates.

Sample	M_n, g/mol [a]	M_w/M_n [a]	ζ, mV	DS [b]	Peptide mass fraction, % [b]
CS	19,255	1.88	1.15	-	-
CSNMI	20,928	1.91	1.29	0.19 (0.07)	-
CSOMI	21,910	1.90	1.20	0.27 (0.11)	-
CSNHHC	30,289	2.03	4.57	0.18 (0.05)	45.2 (12.4)
CSOHHC	32,107	1.96	4.73	0.23 (0.06)	47.6 (12.6)

[a] Molecular weight and polydispersity index were derived from the size-exclusion GPC analysis.

[b] Degree of substitution (DS) and peptide mass fraction were experimentally determined from peak area integrations in the corresponding ^{1}H NMR spectrum, while the values in bracket were experimentally determined from the increase of M_n recorded by GPC chromatograms.

Table 2. Antimicrobial activity, hemolytic effect, cytotoxicity and therapeutic index of the polysaccharides and peptidopolysaccharide conjugates.

Sample	MIC, μg/mL [a]				HC_{50} μg/mL	IC_{50} μg/mL	Selectivity [b]			
	E. coli	*P. aeruginosa*	*S. aureus*	*S. epidermidis*			*E. coli*	*P. aeruginosa*	*S. aureus*	*S. epidermidis*
CS	> 2048 [c]	> 2048 [c]	> 2048 [c]	> 2048 [c]	>> 16384 [c]	>> 2048 [c]	-	-	-	-
CSOMI	> 2048 [c]	> 2048 [c]	> 2048 [c]	> 2048 [c]	>> 16384 [c]	>> 2048 [c]	-	-	-	-
CysHHC10	32	64	32	8	> 1024	> 84	> 32 (> 3)	> 16 (> 1)	> 32 (> 3)	> 128 (> 11)
CSNHHC	128 (58)	128 (58)	128 (58)	16 (7)	> 8192	> 215	> 64 (> 2)	> 64 (> 2)	> 64 (> 2)	> 512 (> 13)
CSOHHC	64 (30)	128 (61)	32 (15)	8 (4)	> 4096	> 180	> 64 (> 3)	> 32 (> 1)	> 128 (> 6)	> 512 (> 23)

[a] Values in bracket express the mass of peptide only in the conjugate, calculated based on the peptide mass fraction.

[b] Selectivity values were calculated as HC_{50}/MIC, whereas selectivity values in bracket were calculated as IC_{50}/MIC.

[c] The values were not observed up to the highest concentrations of compound tested (2048 μg/mL for MIC and IC_{50}, 16384 μg/mL for HC_{50}).

Figure 1. ^{1}H NMR spectra of polysaccharides and peptidopolysaccharide conjugates.

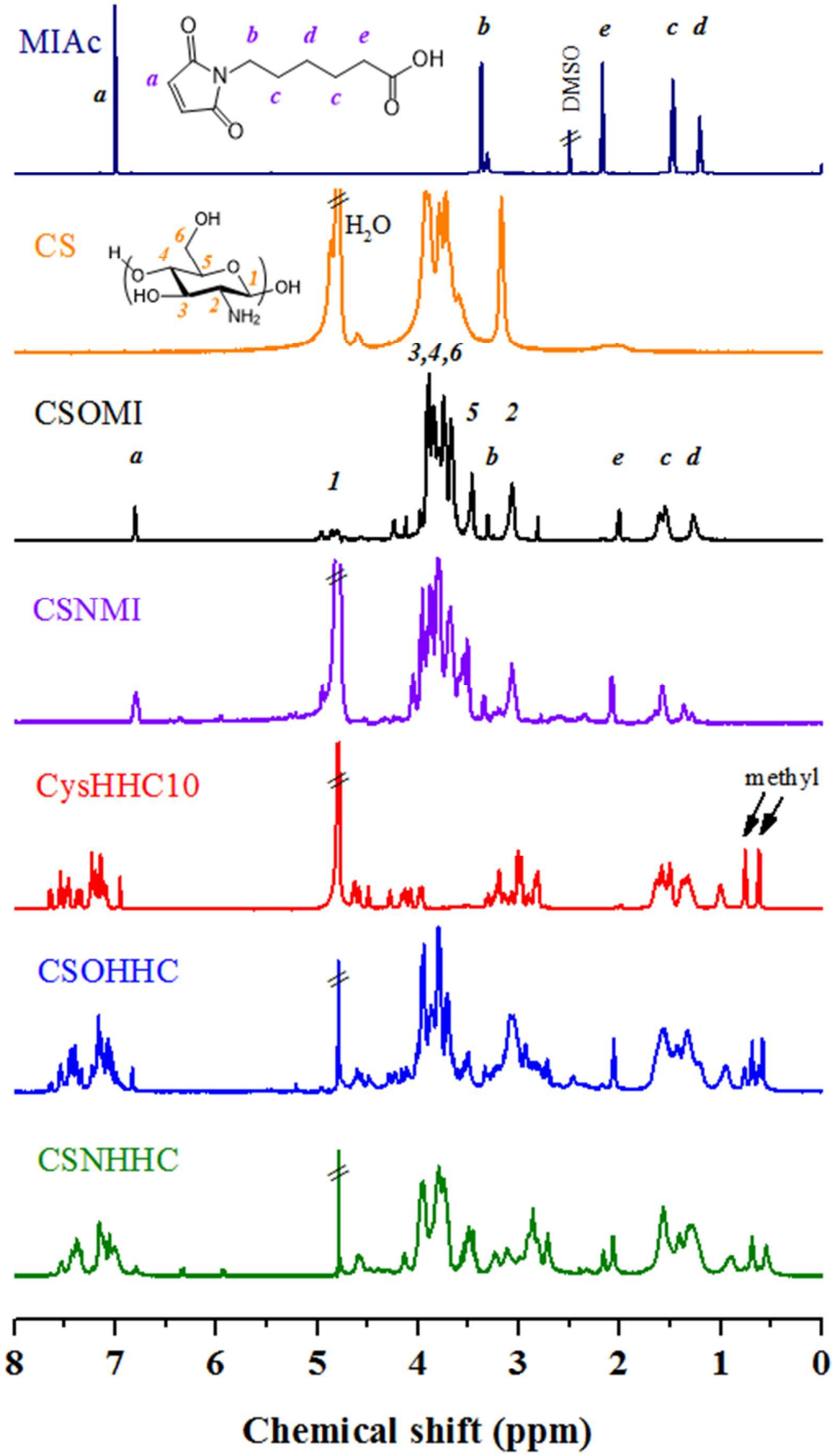

Figure 2. XPS wide-scan spectra of the (a) pristine SS, (b) TA-modified SS, and (c–f) SS surfaces coated with 5- and 10-bilayers of TA and peptidopolysaccharides.

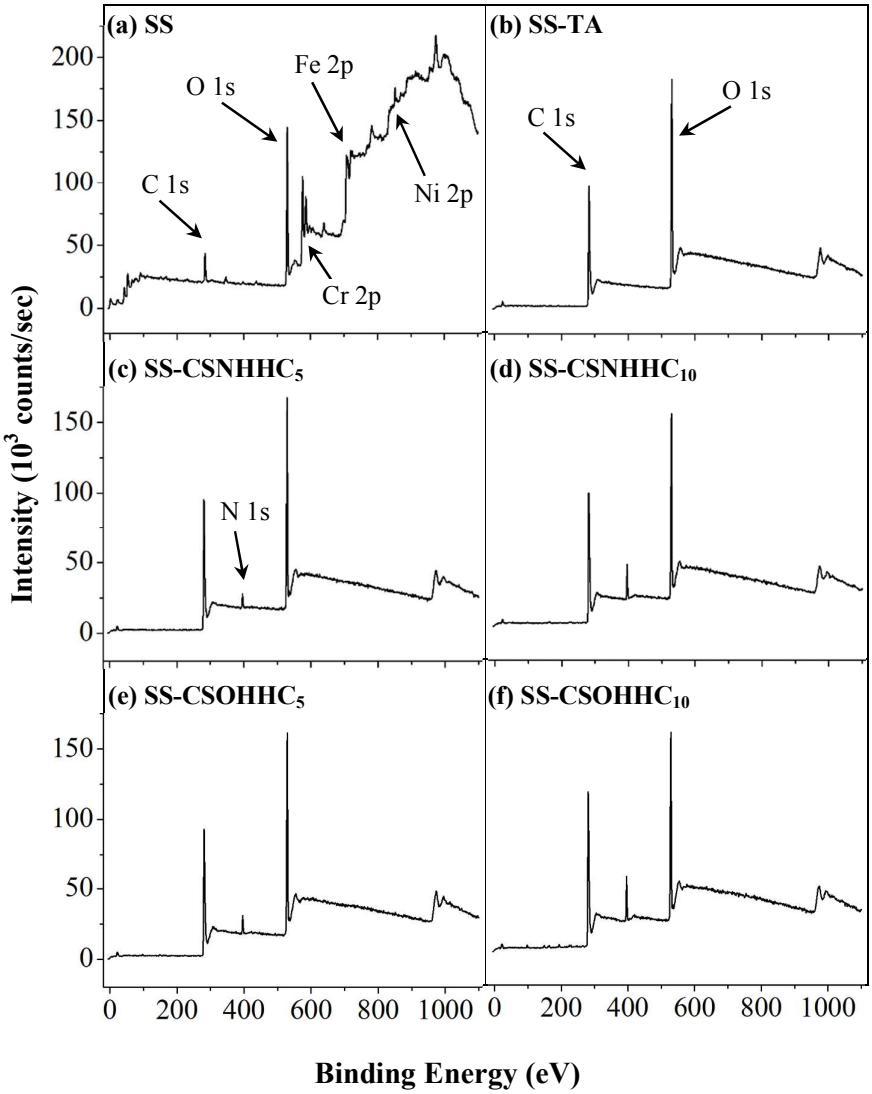

Figure 3. Cross-sectional FESEM images of the (a) pristine SS, (b) SS-CSNHC$_{10}$, (c) SS-CSOHHC$_{10}$ surfaces, and (d) coating thickness of the TA-peptidopolysaccharide bilayers on SS surfaces measured using ellipsometry. Scale bar is 100 nm. Error bar denotes standard deviation obtained from three replicates.

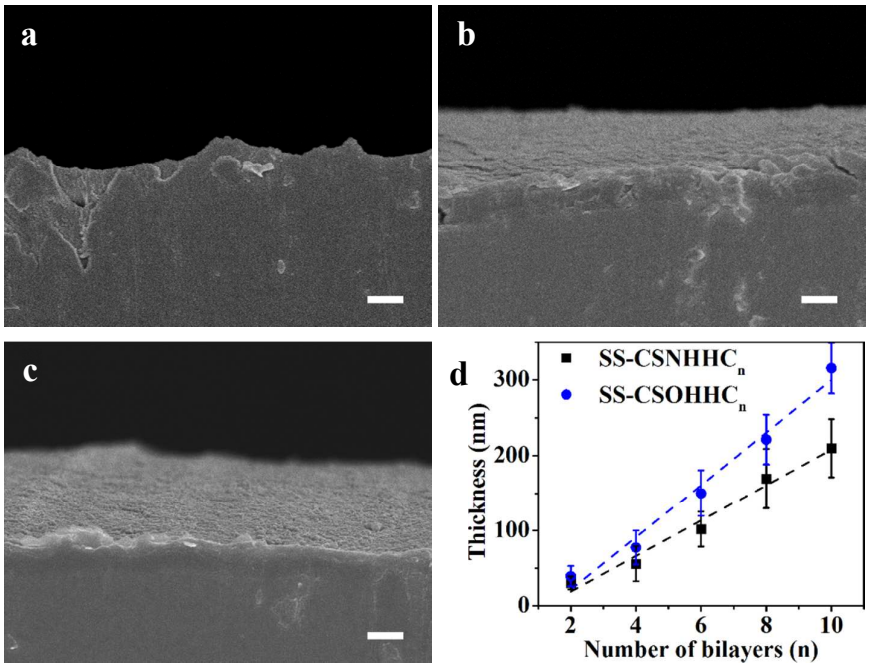

Figure 4. Relative cell viability of the 3T3 fibroblasts after 24-h incubation with the polysaccharides and peptidopolysaccharide conjugates. Error bar denotes standard deviation obtained from three replicates.

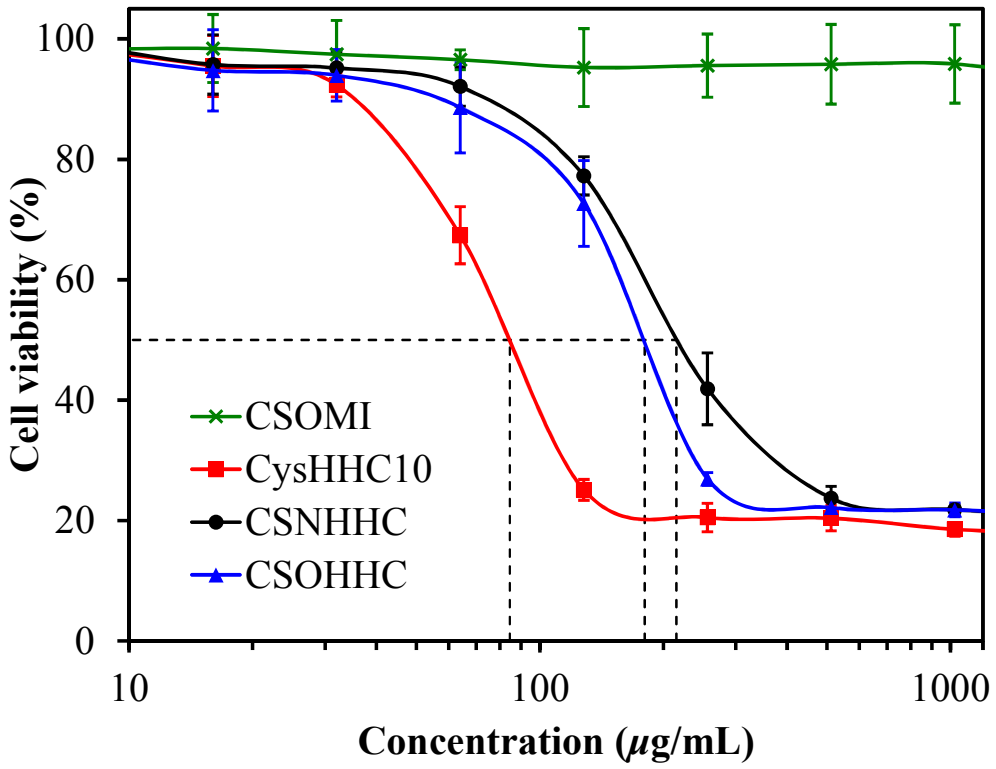

Figure 5. Fluorescence micrographs of live (green) and dead (red) *E. coli* (a–d) and *S. aureus* (e–h) adhered to the (a,e) pristine SS, (b,f) SS-TA, (c,g) SS-CSNHHC$_{10}$, and (d,h) SS-CSOHHC$_{10}$ surfaces after 4-h immersion in the bacterial suspension (10^7 cells/mL) at 37 °C. Scale bar is 50 μm.

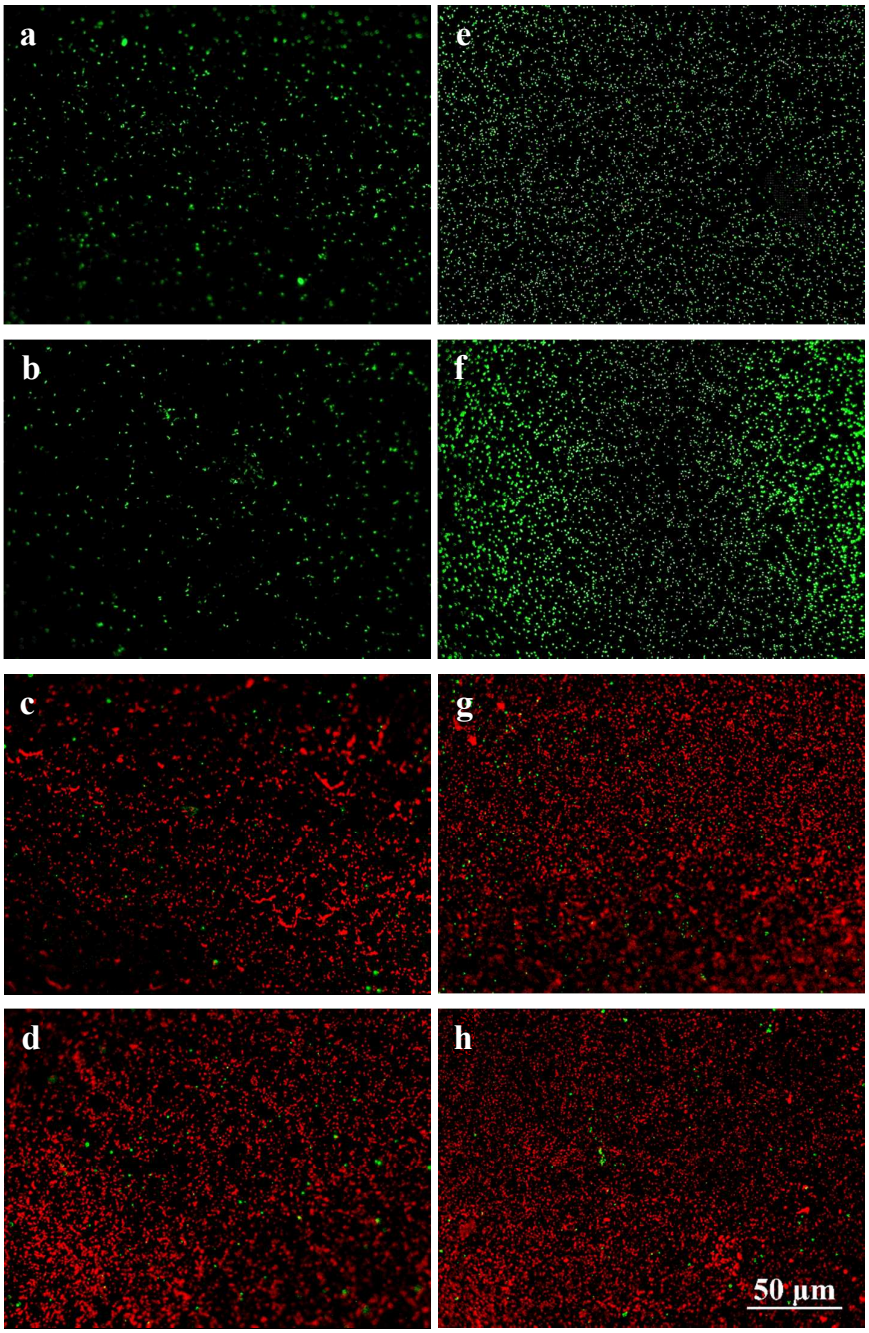

Figure 6. Fluorescence micrographs of 3T3 fibroblasts adhered to the (a) pristine SS, (b) SS-CSNHHC$_{10}$, and (c) SS-CSOHHC$_{10}$ surfaces after 24-h immersion in the cells suspension (2×10^5 cells/mL) at 37 °C and (d) their relative count of cell viability. Scale bar is 200 μm. Error bar denotes standard deviation obtained from three replicates. Asterisk (*) denotes significant difference with p-value < 0.05 (Tukey's test).

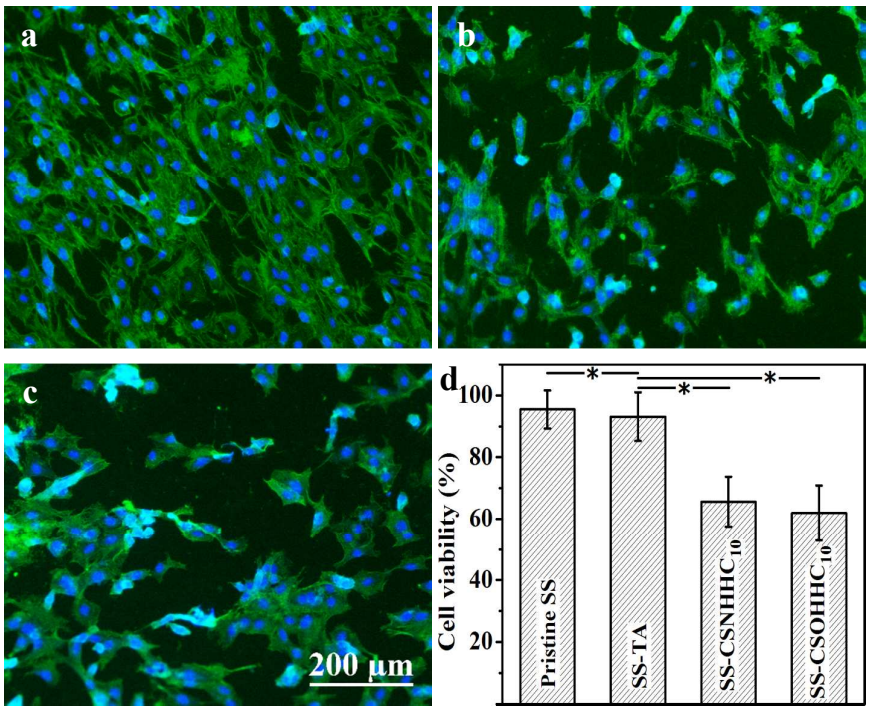

TOC Graphic

Title: Chitosan-based Peptidopolysaccharides for Cationic Antimicrobial Agents and Antibacterial Coatings

Authors: Dicky Pranantyo, Li Qun Xu, En-Tang Kang, and Mary B. Chan-Park

Summary/highlights:

Peptidopolysaccharides with peptidoglycan-mimetic structure can target and compromise microbial membrane with moderate hemo- and cytotoxicity, potentially applicable as antibiotics and antimicrobial coatings.